http://dx.doi.org/10.5012/bkcs.2012.33.5.1748

Tip-Enhanced Raman Scattering with a Nanoparticle-Functionalized Probe

Chan-Gyu Park, Ju-Young Kim, Eunbyoul Lee, Han-Kyu Choi, Won-Hwa Park,† Jinwook Kim, and Zee Hwan Kim*

*Department of Chemistry, Korea University, Seoul 136-701, Korea. *E-mail: zhkim@korea.ac.kr*
†Emerging Technology R&D Lab, LG Electronics, Seoul 137-724, Korea
Received January 20, 2012, Accepted February 27, 2012

We carried out the tip-enhanced Raman scattering (TERS) with a tip that is functionalized with a Au-nanoparticle (AuNP, with a diameter of 250 nm). The AuNP tip is fabricated by a direct mechanical pickup of a AuNP from a flat substrate, and the TERS signal from the AuNP tip - organic monolayer - Au thin film (thickness of 10 nm) is recorded. We find that such a AuNP-tip interacting with a thin film routinely yields signal enhancement larger than ~10^4, which is sufficient not only for local (with detection area of ~200 nm^2) Raman spectroscopy, but also the nanometric imaging of organic monolayers within a reasonable acquisition time (~20 minutes/image).

Key Words : Plasmons, Nanoparticles, Raman scattering

Introduction

The tip-enhanced Raman scattering (TERS)[1-7] is a variation of surface-enhanced Raman scattering (SERS) in which stationary nanoparticles and nanostructures in the sample surface are replaced by a "mobile" scanning probe. Because of its close connection to SERS, the researchers naturally have expected that the TERS will eventually provide the structure-specific detection of organic molecules at a single-molecule sensitivity and a nanometric chemical imaging. However, a full experimental realization of such expectation is proved to be a major challenge, and currently the successful TERS is possible only for a limited set of target systems, including single-wall carbon nanotubes,[4] organic monolayers,[1] and organic dye molecules.[6]

The most important quantity in TERS is the enhancement factor, $EF = |E/E_0|^4$, where the E is the locally enhanced field at the extremity of the tip and the E_0 is the incident field. In theory, an idealized Au-tip with conical shape should provide $EF = 10^5$ even without the tip-substrate interaction.[8] However, the surfaces of real metal-coated or monolithic metal tips are by no means smooth, and this non-ideality results in significantly lower enhancements in real experimental situation. To increase the EFs for more useful TERS, many researchers have attempted to fabricate the tip that natively possess metallic gap structures, such as bow-tie antennas[9] or coaxial nanostructures,[7] yet even these elaborately engineered tips do not alwaysprovide EFs partly because of the current technical barrier of nano-fabrication.

Here we demonstrate a simple experimental strategy for TERS that routinely provides signal enhancement larger than $EF = 10^4$. Our strategy is based on the coupled plasmon mode of a gold nanoparticle (AuNP) - gold thin film (AuTF) junction, which is known to provide fairly reproducible and strong SERS enhancements ($EF > 10^5$).[10] In the current work, a AuNP attached at the end of a tip serves as the TERS tip, and the enhanced Raman signal from the tip - molecules - AuTF structure is detected. Aside from the enhancement factors, what distinguishes our TERS from the previous ones is that we were able to carry out the TERS measurements under the non-contact mode. Unlike the TERS that is based on contact mode, the TERS under non-contact mode operation does not severely suffer from the frequent tip damage or contamination, allowing for routine measurements. In addition, the non-contact mode is fully operational in the aqueous media. Thus, we expect that the current strategy can be even adapted to many interesting "wet-surfaces" such as electrochemical surfaces or supported lipid bilayers. Below, we show that this method allows one to easily obtain TERS spectra of ~100 of Raman-active molecules on metallic surfaces, but it also enables one to spectroscopically image the sample surface with a spatial resolution better than 70 nm.

Method

The TERS microscope is essentially a combination of an inverted microscope (IX71, Olympus), a Raman spectrometer (Triax 320, Horiba; DU-401, Andor Tech), and an atomic force microscope (AFM, XE-120, Park systems). Linearly polarized light from a HeNe laser (~1 mW) is injected to the entrance port of the inverted microscope and is focused onto the tip-sample junction through a high-NA objective lens (oil immersion type, NA = 1.46) and the back-scattering from the tip-sample junction is collected by the same objective lens. The collected scattering is filtered through a dichroic Raman beam splitter and an edge filter and is fed into the spectrometer (Figure 1). The AFM operates under non-contact mode in which the tip-end scans 1-2 nm above the surface when the feedback is engaged. The sample is a monolayer of 4-methylbenzenethiol (MBT) self-assembled on the surface of a Au thin-film (with a thickness of 10 nm) formed on a glass coverslip. The colloidal gold nanoparticle (AuNP) with a diameter of 250 nm is purchased from the

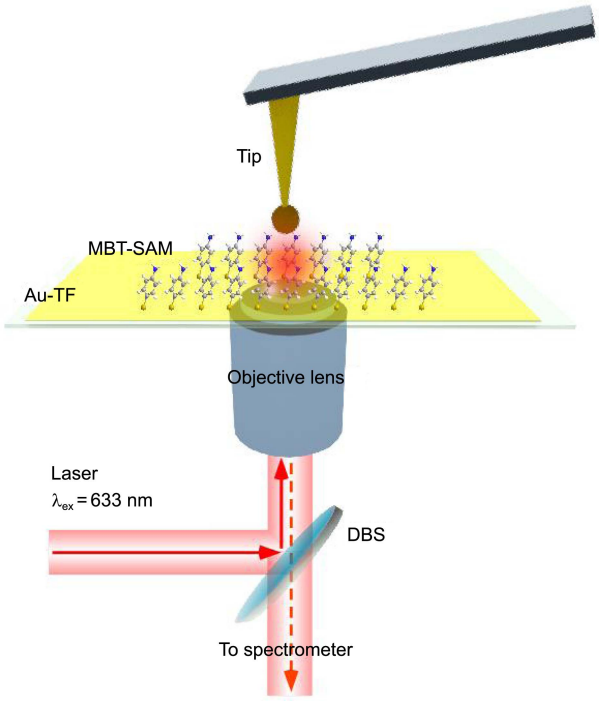

Figure 1. The schematic diagram of the TERS microscope.MBT-SAM = self-assembled monolayer of 4-methylbenzenethiol; AuTF = gold thin film with a thickness of 10 nm; DBS = dichroic Raman beam splitter.

British Bio-cell International Corp, and is dispersed on a cleaned glass coverslip for the particle pick up experiment (see below for detail).

Results and Discussion

Before we move onto the experimental results, we first explain why we specifically chose the nanoparticle-tip (NP-tip) as a TERS tip, instead of more usual monolithic metal tips[4] or metal-coated dielectric tips.[3] These conventional tips are fabricated by the etching of metallic wire or evaporative deposition of metals, which necessarily produce rough surfaces. The roughness of the tip-end usually generates SERS signals when organic contaminants are accidentally adsorbed, which acts as background in TERS measurements. Furthermore, all metallic tips (usually provide the highest EFs) are not experimentally compatible with a normal AFM operation because it cannot withstand the mechanical stress of contact mode or non-contact mode in AFM feedback conditions. We expect that a AuNP (single crystalline) placed at the extremity of an AFM tip (AuNP-tip) will not generate SERS background and it is compatible with normal AFM operations. Here we consider only the electromagnetic-enhancement mechanism, which approximately scales with the fourth power of the locally enhanced field (EF = $|E / E_0|^4$, where E is the locally enhanced field and E_0 is the incident field). As pointed out by Halas and Nordlander group[11,12] the NP-TF junctions possess two resonances: the isolated dipole resonance of a nanoparticle and coupled NP-TF resonance.

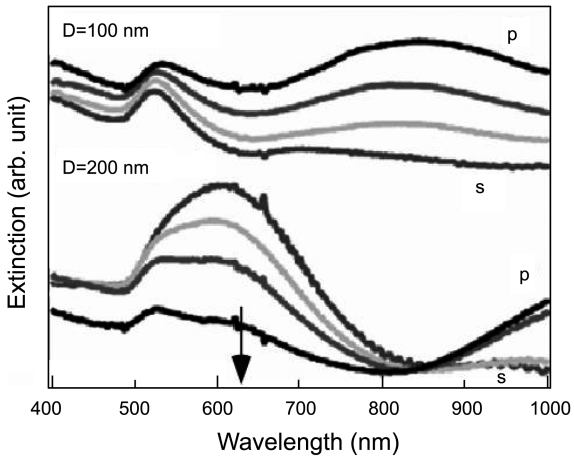

Figure 2. The ensemble-averaged extinction spectra of AuNP -4-aminobenzenethiol monolayer-AuTF. Upper spectra: AuNP with a diameter = 100 nm, lower spectra: AuNP with a diameter of 200 nm. In both the sample, the thickness of the AuTF is 20 nm and the gap-distance is 0.7 nm as defined by the physical dimension of aminobenzenethiol monolayers. The multiple spectra are obtained with varying incidence angle of light with respect to the sample surface such that the amount of s- and p-components of the light are introduced to the sample surface. The arrow points to the TERS excitation wavelength of 633 nm.

The latter resonance is expected to cause greater EF than the former. Figure 2 shows one such example of dual-resonance occurring in NP-TF junction. The extinction spectra of AuNP (100 nm diameter) - 4-aminobenzenethiol - AuTF (thickness of 20 nm) has isolated resonance near 530 nm, while the coupled resonance occurs near 800 nm. Increase in particle diameter, reduction in gap-distance, or reduction in the thickness of TF lead to red-shift of the coupled resonance. In particular, with a junction with a particle diameter of 200 nm and a film thickness of 20 nm, the coupled resonance wavelength is already > 1,000 nm (see the lower panel spectra of Figure 2). In our particular experimental condition, diameter of AuNP is 250 nm and the thickness of the film is 10 nm. Thus, the excitation wavelength of 633 nm employed in the current experiment is not fully resonant with the coupled resonance. The fine-tuning of the resonances in TERS will be a subject of further research, yet we point out that even with off-resonant excitation, we could obtain sufficient TERS signals.

The Figure 3 compares the simulated (at the excitation wavelength of 633 nm, finite-difference time-domain, FDTD, method) field enhancements for a Au thin film interacting with tips with two different shapes.The gap-distance in the simulation is set at 3 nm while the experimental condition is less than 1 nm just to reduce the computational efforts in the simulation, and thus the simulation is only qualitatively correct. Nevertheless, the simulation shows the design rule for the tip.With p-polarized excitation, the AuNP tip -AuTF junction produces EF of ~10^7 (Figure 3(a)). Addition of a thin Au-coating on Si-structure of the AuNP-tip (Figure 3(b)) only slightly lowers the EF. We find that these EFs are comparable to those of monolithic, all-metallic Au-tips. As

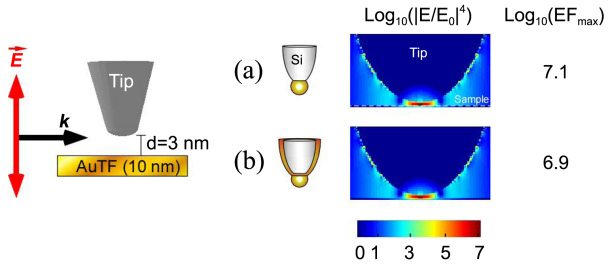

Figure 3. FDTD simulation results of local enhancement (log scale, $Log_{10}(|E/E_0|^4)$, E = local field, E_0 = incident field) between a Au thin-film (thickness of 10 nm) and TERS probes with twodifferent shapes. (a) AuNP (diameter of 250 nm)-terminated Si-tip; (b) same as (a), but with a thin coating (5 nm) on Si-tip. In the simulations, the incident excitation at λ = 633 nm is polarized along the tip axis and the tip-sample distance is fixed at d = 3 nm. Also shown in the right are the maximum enhancements ($Log_{10}(EF_{max})$) for given configurations.

discussed below, the thin Au-coating on Si-tip serves as a "glue" that holds the AuNP in place. Note that in our experiment, we illuminate the laser beam normal to the sample surface through a high-NA objective lens. Only the high-NA component of the input beam (*i.e.*, portion of laser beams that makes large angle from the surface normal) will drive the TERS signals. Thus, the simulated EF values do not precisely reflect the experimental conditions. However, it serves as a qualitative guideline for the design of TERS probe.

The NP-tip fabrication is carried out in three steps (see Figure 4). First, an etched Si-tip (tapping mode, resonance frequency of ~300 kHz, Nanosensors) is mechanically ground against a Si-wafer surface to make a flat (or blunt) end-surface. This step ensures the tip-end to make sufficiently large contact area with the nanoparticle, enhancing the success rate for the particle pickup. Second, the tip is coated with a thin layer of Au (thickness of 5 nm) and Ti (thickness of 1 nm, serves as an adhesion layer between Si and Au surfaces). The Au-coating on the tip acts as a "glue" that can pickup and hold the AuNP (see below) by forming a covalent metallic bridge between the AuNP and the tip-end. This Au-Au "glue" effect is well known in molecular electronics,[13] in which soft metals such as Ag or Au can form metallic bonds simply by applying mechanical pressure. Bare Si-AFM tip can sometimes pick up the AuNP from the surface *via* a electrostatic interaction, yet the probability is too low to be useful.

As described above, metallic coating on the tip may reduce the local field intensities, and one could instead use organic linkers (such as polyethylenimines or poly-L-lysines) to functionalize the tip in order to pick up the NPs. However, we find that such organic likersare not as stable as the metallic bridge, and they often generate unwanted Raman or SERS signals of linker molecules.

In the last step of the fabrication, a nanoparticle is attached to the tip-end *via* the mechanical pickup. The Figure 4(a) describes the details of the pickup process. By carrying out a usual AFM topography measurement on AuNPs dispersed

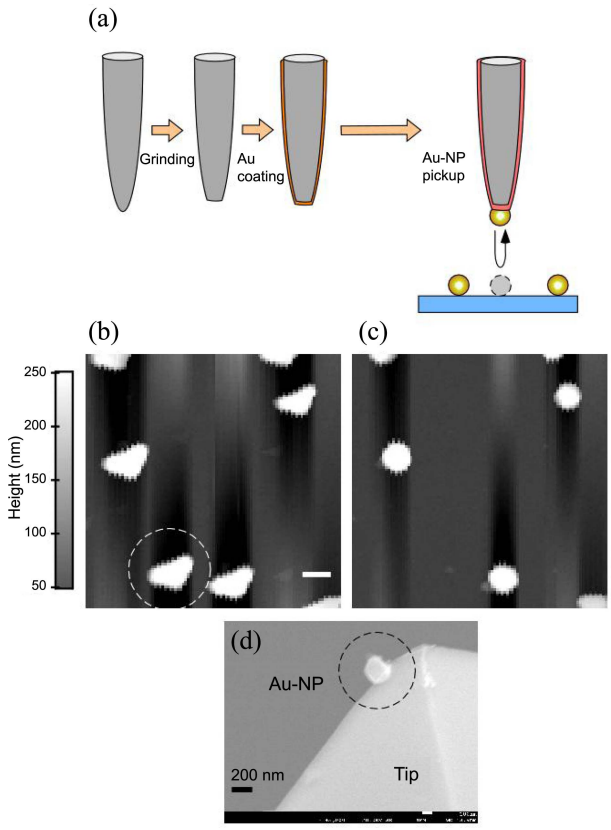

Figure 4. (a) Fabrication procedure of the AuNP-tip; (b) AFM topography before the pickup; (c) AFM topography after the successful pickup. The dashed circle points to the position of AuNP picked up by the tip. The scale bar in (b) corresponds to 500 nm scale. (d) A representative scanning electron microscopy (SEM)-image of a AuNP-tip fabricated by the pickup procedure described in the main text.

on glass substrate, we first locate the NPs, and the tip is "hard-landed" on top of a nanoparticle. The hard-landing is achieved by temporarily switching the feedback of AFM from non-contact-mode to the contact-mode so that the tip and nanoparticle experience large mechanical force of > 600 nN. The tip is then retracted from the surface to form AuNP-tip. The success of pickup event can be readily verified by comparing the topography before and after the hard-landing. Figures 4(b) and 4(c) show an example of topography change that signals a successful pickup, in which one nanoparticle disappears and the topographic shapes of each nanoparticles are drastically changed. The triangular shapes in Figure 4(b) (before the pickup) are the result of the triangularly shaped tip-end interacting with the near-spherical nanoparticles. After the successful pickup, the triangular motifsare changed to spherical ones (Figure 4(c)) because the picked up AuNP now serves as a tip-end. Figure 4(d) shows a scanning electron microscopy (SEM) image of a typical AuNP-tip. The procedure allows us typically success rate exceeding 80%. After the pickup process, the nanoparticle maintains contact with the tip-end that is stable for at least 1 day.

Figure 5(a) shows TERS spectra (exposure time of 10

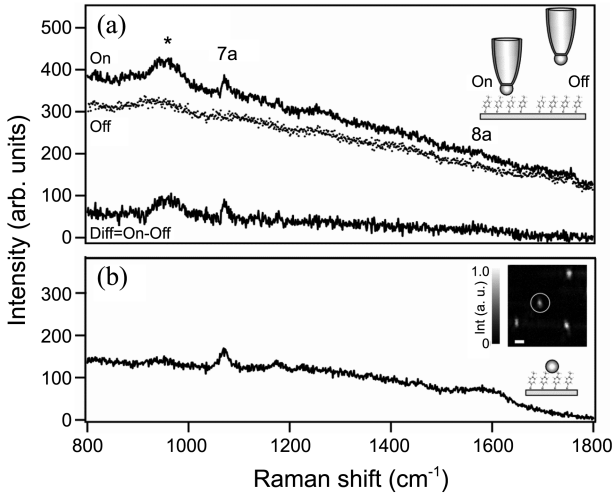

Figure 5. (a) The TERS spectra of MBT with the NP-tip engaged on the sample surface (on, thick line), with the NP-tip retracted from the surface (off, dotted line), and the difference (on-off, thick line) between the two. The peak assignment of the 7a (1072 cm^{-1}) and 8a (1583 cm^{-1}) modes of MBT is based on Rycenga *et al.*[14] The exposure time for obtaining the TERS spectra is 10 seconds. The peak near 960 cm^{-1} (mark as *) is the 2nd order Raman scattering of the Si-tip. (b) The SERS spectrum from a self-assembled AuNP-MBT-AuTF junction. The exposure time for the acquisition of the spectrum is 1 second. The inset data is a confocal Rayleigh scattering image of the AuNP-MBT-AuTF sample, in which each bright spots represents isolated AuNPs. The scale-bar in the image is 1 μm.

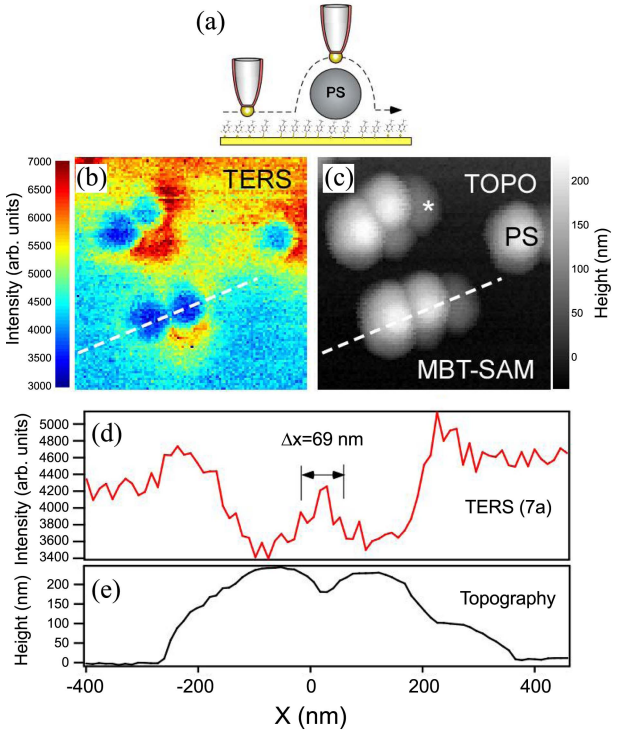

Figure 6. (a) Schematic of the PS-sphere/MBT-SAM/AuTF sample interacting with a AuNP-tip. (b) TERS intensity map of the sample monitoring the 7a (1072 cm^{-1}) mode of MBT. (c) Simultaneously acquired AFM topography. The scan ranges for the TERS and AFM images are 1.5 μm by 1.5 μm. In the image PS-spheres appear as white balls. The asterisk mark (*) points to the topographic artifact (tip-convolution) (d, e) the line profiles of TERS intensity and topography sampled from the dashed lines in (b) and (c). The Δx is an estimate of spatial resolution as determined from the fwhm of a feature in the line profile.

seconds for each) of 4-methylbenzenethiol (MBT) monolayers on AuTF, taken with the NP-tip engaged on sample surface (on), with the tip retracted from the surface (off), and the difference between the two (diff = on-off). Aside from the 2nd order silicon Raman phonon peak from the Si-tip (~960 cm^{-1}), the most apparent feature is the 7a (1072 cm^{-1}) peak of the MBT.[14] The intensity of 8a-peak is too weak as compared with the noise level in the difference spectrum. The retraction of the tip, or the retraction of sample surface from the laser focus lead to the disappearance of peaks of MBT, confirming that the signal does not originate from the SERS of MBTs accidentally adsorbed on NP-tip, or from the native SERS of MBTs on AuTF surface.

We find that the TERS intensities of MBT are consistently smaller than those of SERS from a self-assembled AuNP-MBT-AuTF junction by a factor of ~10, even though the two are based on exactly the same metallic structure. An example of such difference is shown in Figure 5(b). The SERS spectrum shown in Figure 5(b) is obtained from aAuNP-MBT-AuTF junction. We can easily verify that only one AuNP is located within a focus area by the bright spots with regular intensities in confocal Rayleigh scattering image. The SERS spectrum is obtained by placing a laser focus on such spots (circle in the inset image). The SERS spectrum in Figure 5(b) is integrated for 1 second, which is comparable to the TERS spectrum obtained in 10 seconds (Figure 5(a)). This difference can be explained by the presence of Au-coated Si-tip, which, according to the electrodynamic simulation above, slightly decreases the EFs, and from the difference in gap-distances for the two cases. In the self-assembled AuNP-MBT-AuTF junction for SERS, the gap distance, *d*, is about 0.7 nm, which is defined by the molecular size of MBT. For the TERS junction, on the other hand, the non-contact mode operation of the AFM results in extra 1-2 nm tip-sample distance, leading to significantly reduced enhancement in Raman signal. We estimate that the signal enhancement factor for the TERS ~10^4 (as estimated from the intensities of 7a), which is still weaker than that of the SERS counterpart, yet strong enough for high-resolution surface chemical mapping. Figure 5 shows one such example.

The Figure 6 shows the TERS and simultaneously recorded AFM images of a sample. The sample is composed of polystyrene (PS, diameter of 200 nm) spheres dispersed on top of the MBT/AuTF surface (see Figure 6(a)). Each point in the image (Figure 6(b)) corresponds to the intensity of 7a-peak of MBT integrated for 100 ms, andtypical acquisition time for obtaining one TERS image is ~20 minutes.In the image, the PS-spheres appear as negative contrasts, which agree with our expectation that the TERS signal is induced by the strong NP-TF coupling, and the PS-sphere weakens such a coupling by increasing the NP-TF distance.

Figures 6(d) and 6(e) show line-profiles of TERS and AFM topography images sampled from Figures 6(b) and 6(c), which show high spatial resolution (negative) contrasts of two adjacent PS-spheres. From the line-profile, we estimate that the spatial resolution Dx of the TERS image is about 70 nm. It might be wondered how one could obtain a spatial resolution better than the geometric radius of curvature of the tip-end (in our case, 125 nm, the radius of the AuNP). As is well known (see for example Park *et al.*[10]), the spatial dimension of the enhanced local field formed at the AuNP-AuTF junction is about 10-50 nm. Thus, the spatial resolution can be better than the geometric shape of the tip-end when the tip is strongly coupled to the substrate.

Conclusion

In this work, we demonstrated that a nanoparticle-functionalized tip interacting with a thin metallic film allows one to carry out an efficient TERS measurement on densely packed organic monolayers. While the enhancement is already sufficient for many interesting applications, we believe that there is still plenty of room for the improvement. As mentioned above, the current TERS excitation is not fully resonant with the NP-TF coupled resonance. We expect that the TERS with smaller NP and the excitation wavelength near 800 nm will provide much better signal enhancements.

Acknowledgments. The authors acknowledge the support from Priority Research Centers Program (2011-0018396), SRC (2012-0000606), and Nano R&D program (2011-0019150) through the National Research Foundation of Korea (NRF) funded by the Ministry of Education, Science and Technology.

References

1. Pettinger, B.; Ren, B.; Picardi, G.; Schuster, R.; Ertl, G. *Phys. Rev. Lett.* **2004**, *92*, 096101.
2. Deckert, V. *J. of Raman Spectrosc.* **2009**, *40*, 1336.
3. Hayazawa, N.; Motohashi, M.; Saito, Y.; Ishitobi, H.; Ono, A.; Ichimura, T.; Verma, P.; Kawata, S. *J. of Raman Spectrosc.* **2007**, *38*(6), 684-696.
4. Hartschuh, A.; Sanchez, E. J.; Xie, X. S.; Novotny, L. *Phys. Rev. Lett.* **2003**, *90*, 095503.
5. Verma, P.; Yamada, K.; Watanabe, H.; Inouye, Y.; Kawata, S. *Phys. Rev. B* **2006**, *73*, 045416.
6. Stockle, R. M.; Suh, Y. D.; Deckert, V.; Zenobi, R. *Chem. Phys. Lett.* **2000**, *318*, 131.
7. Weber-Bargioni, A.; Schwartzberg, A.; Cornaglia, M.; Ismach, A.; Urban, J. J.; Pang, Y. J.; Gordon, R.; Bokor, J.; Salmeron, M. B.; Ogletree, D. F.; Ashby, P.; Cabrini, S.; Schuck, P. J. *Nano Lett.* **2011**, *11*, 1201.
8. Yang, Z.; Aizpurua, J.; Xu, H. *J. Raman Spectrosc.* **2009**, *40*, 1343.
9. Weber-Bargioni, A.; Schmidt, M.; Harteneck, B.; Ogletree, D. F.; Schuck, P. J.; Cabrini, S. *Nanotechnology* **2010**, *21*, 065306.
10. Park, W.-H.; Kim, Z. H. *Nano Lett.* **2010**, *10*, 4040.
11. Le, F.; Lwin, N. Z.; Steele, J. M.; Käll, M.; Halas, N. J.; Nordlander, P. *Nano Lett.* **2005**, *5*, 2009.
12. Halas, N. J.; Lal, S.; Chang, W.-S.; Link, S.; Nordlander, P. *Chem. Rev.* **2011**, *111*, 3913.
13. Jang, S. Y.; Reddy, P.; Majumdar, A.; Segalman, R. A. *Nano Lett.* **2006**, *6*, 2362.
14. Rycenga, M.; Camargo, P. H. C.; Li, W.; Moran, C. H.; Xia, Y. *J. Phys. Chem. Lett.* **2010**, *1*, 696.